PET-Fluorodeoxyglucose of Cranial and Spinal Neuromas

Katalin Borbely, Michael J. Fulham, Rodney A. Brooks and Giovanni Di Chiro

Neuroimaging Branch, National Institute of Neurological Disorders and Stroke, National Institutes of Health, Bethesda, Maryland

Five patients with eighth nerve, one with ninth nerve and one with cervical neuromas were studied with PET and [^{18}F] fluorodeoxyglucose (FDG). Four of the patients had had surgery prior to the PET study, and six patients had subsequent surgery. All tumors were well-visualized on the PET images. Only one patient with bilateral acoustic neuroma exhibited tumor recurrence or growth after the PET study; these two lesions showed the highest FDG uptakes in the PET studies (tumor-to-cerebellum ratio of 0.93–0.98). All other tumors were relatively hypometabolic (tumor-cerebellum ratios of 0.43–0.65) and showed no tumor growth or recurrence during follow-up periods ranging from 5 to 8 yr. These results suggest that PET-FDG may be of value in the evaluation of cranial and spinal schwannomas.

J Nucl Med 1992; 33:1931–1934

Neuromas (or, more specifically, schwannomas) originate from Schwann cells of the cranial or spinal nerves. The eighth nerve schwannomas, also called acoustic neuromas, are relatively common (8% of all intracranial tumors) and are found in the cerebellopontine angle (CPA) and internal auditory canal (*1*). They occur sporadically and in association with neurofibromatosis Type 2 (NF2), where the gene has been mapped to the middle of the long arm of chromosome 22 (*2,3*). Neuromas are usually benign but sometimes exhibit aggressive behavior which may lead to recurrence after surgical resection (*4*), and even a fatal outcome (*1*).

The majority of malignant schwannomas present as de novo malignant growths rather than as a secondary anaplastic change of a pre-existing benign schwannoma (*1*). Their clinical course is marked by repeated local recurrence associated with increasing anaplasia. Most unoperated schwannomas appear to grow at relatively slow rates (0.2 cm/yr) (*5*). Cushing first reported that after subtotal resection of acoustic schwannomas, tumor regrowth may not be evident for many years (*6*). Similar results have been found for acoustic neuromas by other investigators, with recurrence rates of 21%–23% over extended years of follow-up (*7–9*).

Positron emission tomography (PET) with fluorodeoxyglucose (FDG) has been successfully used for assessing the malignancy of a variety of tumors (*10–12*). We know of no previous reports of PET studies of schwannomas.

We retrospectively analyzed five cases of eighth, one of ninth and one case of cervical neuromas, gathered during twelve years experience with PET studies of brain tumors. We wanted to answer the questions: Does FDG uptake correlate with pathology? Does it correlate with the clinical outcome? Can we predict tumor growth, or likelihood of tumor recurrence following surgery?

MATERIALS AND METHODS

The files of patients with neuromas who were studied with PET-FDG were reviewed. Seven patients with a well-documented clinical and neuroradiological history of schwannoma were selected. Three of the seven patients had no prior surgery at the time of the PET scan, while four harbored residual or recurrent tumors following prior surgery. Six patients, including the four with prior surgery, had further surgery after the PET study.

PET scanning was performed with an ECAT-II scanner (EG&G ORTEC, Oak Ridge, TN, now Siemens, Inc.) in one patient and with the Neuro-PET scanner in six patients. The ECAT-II scans a single slice with a thickness of 20 mm and resolution of 17 mm (13). The Neuro-PET scans 7 simultaneous slices with 6–7 mm in-plane resolution and 11–12 mm slice thickness (*12,14*). Neuro-PET scans were corrected for random coincidences, attenuation and scatter using previously described methods (*12,15*).

Scanning began approximately 30 min after injection of 92–185 MBq intravenous dose of FDG. The patients with intracranial tumors had their eyes covered and ears plugged, head immobilized with a velcro strap (*11*) and the scan angle was parallel to the cantho-meatal line. "Arterialized" venous blood samples were obtained periodically. In six studies, apparent glucose utilization rates were calculated using the Sokoloff three-compartment model (*16,17*) and nominal values for the rate and lumped constants (*10*). Because these nominal constants are not necessarily valid in tumor tissue, our reported values of "apparent" glucose utilization are to be regarded as estimates, not accurate values. In any case, the clinical meaning and utility of the results rests on relative FDG uptake, not on absolute values of glucose utilization.

Received Mar. 3, 992; revision accepted Jun. 26, 1992.
For reprints contact: Giovanni Di Chiro, MD, Bldg. 10 Room 1C451, National Institutes of Health, Bethesda, MD 20892.

The slice used for analysis included the tumor or tumors and, in the first five intracranial cases, the cerebellum and tips of the temporal lobes. In Patient 6, the slice which best represented the tumor was below the cerebellum temporal lobes, and so a different slice was used to obtain these readings. The slice selected for the cervical tumor (Patient 7) passed through the area of maximal bone erosion as identified in the CT studies. Tumor metabolic activity was measured by placing an 8 mm diameter circular region of interest (ROI) over the maximal radioactivity within the tumor region, which was always visually identifiable on the PET images. Whenever available, MRI and/or CT scans were used to aid with the localization of the tumor region. Rates were also measured in the cerebellar cortex using three similar ROIs in each hemisphere, positioned for maximal reading, and 6 mm diameter ROIs in the white and gray matter of the temporal lobes.

Tumor rates were compared to those of the contralateral cerebellar cortex, except that in Patient 5 only the left cerebellum was used because of the effects of surgery and radiotherapy on the right. The cerebellum is an attractive structure for normalization because in five patients it appeared in the same slice as the tumor and because its large size permits accurate measurement. Tumor rates were also compared with those of the white matter (WM) of the temporal lobe. For the ECAT study (Patient 4), metabolic rates were not available; instead, the ratio of activity concentrations is reported.

The PET results were compared with later clinical and diagnostic developments, which included CT and/or MRI scans. Follow-up periods ranged from a minimum of five to a maximum of eight years.

RESULTS

Ratios of apparent glucose metabolic rates in the tumors to those in the cerebellar cortex and white matter are shown in Table 1. Representative PET images and a brief clinical description are shown for five patients (Fig. 1). When available, contemporaneous CT or MRI images are also shown.

DISCUSSION

Previous studies of gliomas with PET-FDG have shown that high grade tumors exhibit an elevated uptake of FDG that may approach or exceed that of normal gray matter. These high grade (Kernohan classification, grades III and IV) lesions stand out clearly from surrounding white matter. However, low grade gliomas (I and II) have an FDG uptake comparable to that of white matter, and are not visually discernible (*18*). This ease of visual distinction has proven very helpful in the grading of gliomas with PET-FDG.

The situation is somewhat different for cranial and spinal nerve schwannomas. These lesions are extracerebral, occurring in regions normally devoid of FDG uptake. In our study, all tumors were readily seen as distinct foci on the PET images, although in the one patient studied on a low-resolution scanner, the hot tumor area merged into the cerebellar hemisphere. However, this ability to visualize the tumor is not necessarily an advantage, since MRI and CT provide better anatomical delineation. It is rather the ability to measure tumor aggressivity that is the unique potential of PET.

Our results suggest that this capability exists also with neuromas, despite the lack of a surrounding reference tissue. The aggressive recurrent tumors in the patient with NF2 (Patient 3) showed a tumor-to-cerebellum contrast that was 73% greater than the other tumors, while the tumor-to-WM metabolic ratio was about 2.2, compared with 1.45 or less for the others. This behavior vis-a-vis white matter is similar to results obtained for cerebral gliomas (*10*) and is consistent with the natural history of these schwannomas. The correlation of PET-FDG results with the "true" clinical status is striking, considering that several of these patients underwent multiple surgeries which left residual tumors, and the ultimate clinical destiny was not clear for several years.

TABLE 1
Clinical and PET Data on the Seven Neuromas

			Tumor		Metabolic ratio*			
Patient no.	Age	Sex	Size (cm)	Location	Tum-to-Cer	Tum-to-WM	Post-surgery follow-up	Figure
No prior surgery								
1	72	F	1	8th right	0.65	1.44	no surgery, no change in size	1A and B
2	68	M	3.5	8th left	0.65	1.45	no recurrence	1C
3	18	F	3.5	8th left	0.93	2.18	recurrence	1D and E
			2.0	right	0.98	2.23	recurrence	
Prior surgery								
4	57	F	2.0	8th right	0.63†	1.32†	no recurrence	
5	35	F	2.5	8th left	0.51	1.26	residual tumor, no growth	
			2.0	right	0.49	1.21	residual tumor, no growth	
6	38	M	4.0	9th left	0.51	1.43	no recurrence	1F and I
7	68	M	6.0	C2-5 left	0.43	1.40	no recurrence	1G and H

* Ratio of apparent metabolic rates of tumor to cerebellar cortex and to white matter (see text).
† Metabolic rates are not available. Ratio of activity concentration is shown.

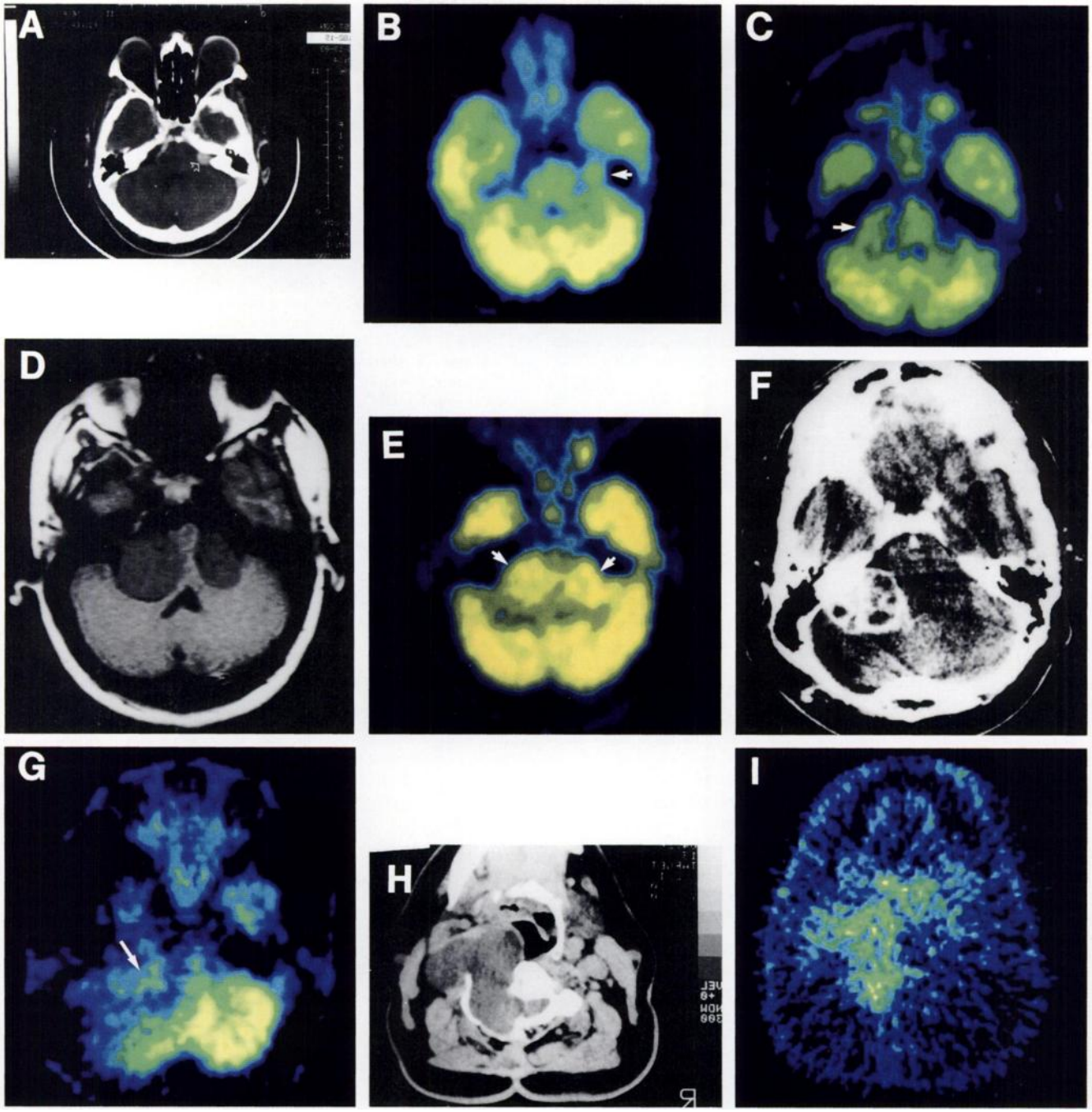

FIGURE 1. (A) Patient 1. A 72-yr-old woman with a 2-yr history of profound right hearing loss and vertigo of recent onset. Postcontrast CT scan shows a rounded, enhancing lesion (open arrow) in the right cerebellopontine angle (CPA). (B) PET-FDG shows a circumscribed focus of increased glucose utilization (arrow) closely corresponding to the tumoral mass in the CT study. (In all CT, MRI, and PET images, the laterality is consistent: right of patient on right of viewer.) (C) Patient 2. A 68-yr-old man with a 5-mo history of left hearing loss and tinnitus. The PET-FDG scan shows an ovoid, circumscribed focus of increased glucose utilization in the left CPA (arrow). CT studies (not shown) demonstrated a 3.5-cm solid, contrast-enhancing left CPA lesion. (D) Patient 3. An 18-yr-old woman with a 10-yr history of neurofibromatosis Type 2. MRI scan shows bilateral CPA mass lesions (L > R). The mass on the left extends into the internal auditory meatus and compresses the fourth ventricle, and both masses compress the brainstem. (E) PET-FDG shows areas of increased glucose utilization (arrows) corresponding to the tumors shown in (D). The tumoral rate of glucose utilization approaches that of the cerebellar cortex. (F) Patient 6. A 38-yr-old man with a 3-yr history of hoarseness and weakness of elevation of left shoulder. Surgery was performed on two occasions (1 and 3 years before PET) with partial removal of a left 9th neuroma. Postcontrast CT shows a heterogeneously enhancing mass in the lateral aspect of the left posterior fossa. The left cerebellar hemisphere is compressed. (G) On PET-FDG of Patient 6, the tumoral metabolism (arrow) contrasts with surrounding hypometabolism, which is probably related to previous surgery and radiotherapy. (H) Patient 7. A 68-yr-old man with a 13-yr history of neck mass (neuronal) which was partially resected in 1971. He had noted increasing weakness and numbness in the left side as well as a change in voice over a 4-mo period. Postscontrast CT shows a large mass eroding the left body and arch of the C3 vertebra and extending into the hypopharynx and soft tissues of the neck. (I) PET-FDG of Patient 7. Note striking correspondence between increased glucose utilization in the cervical soft tissues and the mass demonstrated on the CT scan.

REFERENCES

1. Russell DS, Rubinstein LJ. *Pathology of tumours of the nervous system.* Baltimore: Williams & Wilkins, 1989.
2. Rouleau GA, Wertelecki W, Haines JL, et al. Genetic linkage of bilateral acoustic neurofibromatosis to a DNA marker on chromosome 22. *Nature* 1987;329:246–248.
3. Martuza RL, Eldridge R. Neurofibromatosis 2 (Bilateral acoustic neurofibromatosis). *N Engl J Med* 1988;318:684–688.
4. Sterkers JM, Viala P, Benghalem A. Recurrence of acoustic neurinomas. *Rev Laryngol Otol Rhinol* 1988;109:71–73.
5. Silverstein H, McDaniel A, Norrell H, Wazen J. Conservative management of acoustic neuroma in the elderly patient. *Laryngoscope* 1985;95: 766–770.
6. Cushing H. Tumors of the nervus acusticus and the syndrome of the cerebellopontine angle. Philadelphia: WB Saunders; 1917.
7. Olivecrona H. Acoustic tumors. *J Neurosurg* 1967;86:6–13.
8. Bentivoglio P, Cheeseman AD, Symon L. Surgical management of acoustic neuromas during the last five years. *Surg Neurol* 1988;29:197–104.
9. Valvassori GE, Guzman M. Growth rate of acoustic neuromas. *Am J Otol* 1989;10;3:174–176.
10. Di Chiro G, DeLaPaz RL, Brooks RA, et al. Glucose utilization of cerebral gliomas measured by [^{18}F]fluorodeoxyglucose and positron emission tomography. *Neurology* 1982;32:1323–1329.
11. Di Chiro G, Hatazawa J, Katz D, Rizzoli HV, De Michele DJ. Glucose utilization by intracranial meningiomas as an index of tumor aggressivity and probability of recurrence: a PET study. *Radiology* 1987;164:521–526.
12. Di Chiro G. Positron emission tomography using (^{18}F) fluorodeoxyglucose in brain tumors. *Invest Radiol* 1987;22:360–371.
13. Phelps ME, Hoffman EJ, Huang SC, Kuhl DE. ECAT: A new computerized tomographic imaging system for positron-emitting radiopharmaceuticals. *J Nucl Med* 1978;19:635–647.
14. Di Chiro G, Brooks RA, Sank VJ, et al. The Neuro-PET: a new high-resolution 7-slice positron emission tomograph. *J Nucl Med* 1982;23:59.
15. Brooks RA, Friauf WS, Sank VJ, Cascio HE, Leighton SB, Di Chiro G. Initial evaluation of a high resolution positron emission tomograph. In: Greitz T, ed. *The metabolism of the human brain studied with positron emission tomography.* New York: Raven Press; 1985:57–68.
16. Sokoloff L, Reivich M, Kennedy C, et al. The (^{14}C)deoxyglucose method for the measurement of local cerebral glucose utilization: theory, procedure, and normal values in the conscious and anesthetized albino rat. *J Neurochem* 1977;28:897–916.
17. Brooks RA. Alternative formula for glucose utilization using labeled deoxyglucose. *J Nucl Med* 1982;23:538–539.
18. Patronas NJ, Di Chiro G, Kufta C, et al. Prediction of survival in glioma patients by means of positron emission tomography. *J Neurosurg* 1985; 62:816–822.

SELF-STUDY TEST

Skeletal Nuclear Medicine

Questions are taken from the *Nuclear Medicine Self-Study Program I,* published by The Society of Nuclear Medicine

DIRECTIONS

The following items consist of a heading followed by numbered options related to that heading. Select those options you think are true and those that you think are false. Answers may be found on page 1993.

You are shown images from a bone scan performed with ^{99m}Tc MDP (Fig. 1). Which of the following are reasonable explanations for the scintigraphic findings?

1. Use of highly deoxygenated, preservative-free saline to dilute the radiopharmaceutical
2. Excessive Al^{+3} breakthrough in the eluate from the technetium generator
3. Excessive free reduced ^{99m}Tc in the radiopharmaceutical
4. The presence of gentisic acid in the radiopharmaceutical
5. Excessive free ^{99m}Tc pertechnetate in the radiopharmaceutical

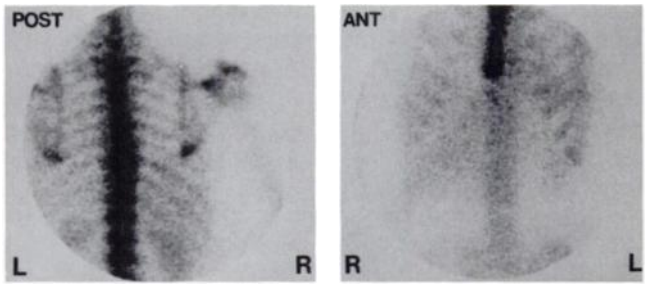

FIGURE 1.

This 62-year-old man has bronchogenic carcinoma. You are shown selected images from a bone scan with ^{99m}Tc MDP (Fig. 2). Reasonable explanations for the findings in the urinary tract include which of the following?

6. Recent chemotherapy
7. Hypercalcemia
8. Obstructive uropathy
9. Renal metastases
10. Iron overload

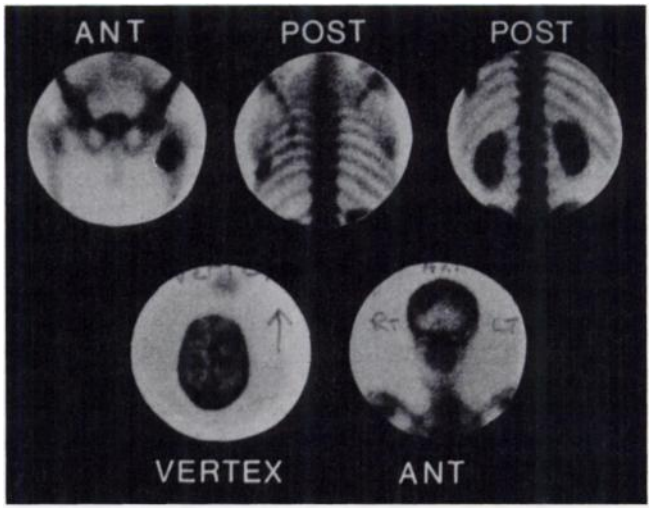

FIGURE 2.

This child has left hip pain. Plain radiographs were normal. You are shown pinhole images of the hips obtained with ^{99m}Tc MDP (Fig. 3). Diagnoses that should be considered, based on the scintigraphic findings, include which of the following?

(continued on page 1993)